CONFIDENTIAL

NASA TM X-550

TECHNICAL MEMORANDUM

X-550

DIRECTIONAL AND LATERAL STABILITY CHARACTERISTICS OF A WINGED REENTRY VEHICLE AT HYPERSONIC SPEEDS

By Charles L. Ladson

Langley Research Center
Langley Air Force Base, Va.

NATIONAL AERONAUTICS AND SPACE ADMINISTRATION
WASHINGTON
August 1961

CONFIDENTIAL

NATIONAL AERONAUTICS AND SPACE ADMINISTRATION

TECHNICAL MEMORANDUM X-550

DIRECTIONAL AND LATERAL STABILITY CHARACTERISTICS OF A WINGED REENTRY VEHICLE AT HYPERSONIC SPEEDS*

By Charles L. Ladson

SUMMARY

An investigation has been carried out at hypersonic speeds to study the directional and lateral stability characteristics of a winged reentry vehicle at high sideslip angles at a Mach number of 9.6 and at high angles of attack (up to a maximum lift coefficient) at a Mach number of 6.7. The effects of rolling the tip fins out from the vertical were also studied at the higher angles of attack.

An analysis of these data showed that if the body shock intersects the wing leading edge inboard of the vertical-tip fins higher directional stability was obtained than if the shock was outboard of the fins. However, as sideslip angle is increased and the shock moves outboard of the tip fin, this increase in stability due to the shock interaction on the fin no longer exists and a decrease or loss in positive directional stability can result. Simple shock-expansion theory gave adequate prediction of the incremental yawing-moment and side-force contributions of the vertical fins for the case where no shock interactions occurred; where shock interaction did occur the theory gave conservative estimates.

At a Mach number of 6.7, rolling the tip fins out 15° and 30° increased the directional-stability level over that for the vertical-tip fins at high angles of attack, but the incremental increase was less than predicted by Newtonian theory. The configuration with vertical-tip fins was directionally stable at all angles of attack up to 60°.

INTRODUCTION

Winged lifting configurations which are being considered for reentry are expected to operate at angles of attack up to that for

*Title, Unclassified.

maximum lift coefficient or about 60°. Over this entire angle-of-attack range it is desirable that the vehicle be not only longitudinally stable and controllable but also have lateral and directional stability. Limited data in this angle-of-attack range at hypersonic speeds have pointed out several problem areas. In references 1 and 2 it is shown that at an angle of attack of 0° a cranked-wing vehicle undergoes a loss in directional stability as the sideslip angle increases due to the body-shock interaction on the vertical-tip fins of the vehicle. Reference 1 also indicated that the directional stability decreased to near zero at angles of attack of about 25° and could become negative at higher angles of attack. Reference 3 presented calculations showing the increase in directional stability which could be obtained at high angles of attack by rolling the tip fins out from the vertical.

The primary purpose of this investigation was to examine the effects of body-fin shock interaction on the loss in directional stability and to determine the effects of wing planform on this phenomenon at a Mach number of 9.6. The secondary purpose of the investigation was to experimentally verify the calculated gain in directional stability due to fin rollout presented in reference 3. This phase of the investigation was undertaken at a Mach number of 6.7.

SYMBOLS

b span, in.

$\bar{c}$ mean aerodynamic chord, in.

C_l rolling-moment coefficient about body center line, $\frac{\text{Rolling moment}}{qSb}$

C_n yawing-moment coefficient about moment center at $0.64l$, $\frac{\text{Yawing moment}}{qSb}$

C_Y side-force coefficient, $\frac{\text{Side force}}{qS}$

C_{l_β} rate of change of rolling-moment coefficient with angle of sideslip at zero sideslip angle, $\left(\frac{\partial C_l}{\partial \beta}\right)_{\beta=0^\circ}$

C_{n_β} rate of change of yawing-moment coefficient with angle of sideslip at zero sideslip angle, $\left(\frac{\partial C_n}{\partial \beta}\right)_{\beta=0^\circ}$

C_{Y_β} rate of change of side-force coefficient with angle of sideslip at zero sideslip angle, $\left(\frac{\partial C_Y}{\partial \beta}\right)_{\beta=0^\circ}$

l body length, in.

$(L/D)_{max}$ maximum lift-drag ratio

M Mach number

q dynamic pressure, lb/sq in.

R Reynolds number based on body length

r radius, in.

S reference area (total projected area of vehicle), sq in.

α angle of attack, deg

β angle of sideslip, deg

Δ incremental value

ϕ fin rollout angle, deg

MODELS AND DESIGNATIONS

The models used are the same as those in reference 1. Drawings showing the dimensions as well as wing planform areas, spans, and mean aerodynamic chords are presented in figure 1. The various models are designated by letter symbols and subscripts and are identified as follows:

B_1 body, shown in figure 1 and the same for all models tested

W_1 74.25° swept clipped-tip delta wing shown in figure 1

W_2 60° swept clipped-tip delta wing shown in figure 1

W_3 68°, 60° cranked leading-edge clipped-tip delta wing shown in figure 1

W_4 76°, 60° cranked leading-edge clipped-tip delta wing shown in figure 1

V_1 40° swept leading-edge upper vertical tail shown in figure 1

The models were constructed of stainless steel and had flat-wing lower surfaces. The nose portion was deflected upward 5° to provide trim angles of attack near $(L/D)_{max}$, and the vehicle incorporated 5° wedge-section vertical-tip fins toed in 5° to provide directional stability. The model nose was blunted to a radius of 0.09 inch and all leading edges had a radius of 0.024 inch normal to the leading edge. The chord of the vertical fins used on the W_4 wing was slightly longer than that on the other planform. This difference resulted in a 9.8 percent larger area for this fin on W_4 than on the other three wings.

For the tests at the higher angles of attack at $M = 6.7$, a 0.850-scale model of configuration $B_1W_1V_1$ was constructed to alleviate a tunnel blockage problem encountered with the larger model. This 0.850-scale model was identical in geometry with the configuration shown in figure 1 with the exception of the vertical-tip fin section which was changed from a blunted 5° wedge to a 0.050-inch-thick blunted flat plate. These tip fins were tested in the vertical position and rolled out 15° and 30° from the vertical.

APPARATUS, TESTS, AND PROCEDURES

Data contained in this report were obtained at Mach numbers of 6.7 and 9.6 in the Langley 11-inch hypersonic tunnel. All force tests were made using internal strain-gage balances. The angles of attack of the models were measured optically by use of a light beam reflected from the model onto a calibrated scale. This method gave the true angles of attack of the model including the deflection of the balance and sting under load. The Reynolds number based on model length for tests at both Mach numbers was 0.6×10^6. At $M = 9.6$, tests were made at sideslip angles from 0° to about 10° at angles of attack of 0° and 10°. At $M = 6.7$, tests were made at sideslip angles from -3° to 10° and at angles of attack from 20° to 60°; however, only the slopes of the data are presented.

RESULTS AND DISCUSSION

Schlieren Flow Photographs

Typical schlieren flow photographs of the flow about the four wing planforms at $\alpha = 0^\circ$ and $M = 9.6$ are shown in figure 2 for several sideslip angles. On the full delta-wing model with wing and body vertexes coincident ($B_1W_1V_1$, fig. 2(a)) the body shock lies outboard of the tip fins at all sideslip angles. However, for configurations $B_1W_2V_1$, $B_1W_3V_1$, and $B_1W_4V_1$ (figs. 2(b), 2(c), and 2(d)) the body shock wave intersects the wing leading edge inboard of the tip fins and moves outboard of the leeward fin as the sideslip angle is increased. Figure 3 presents the schlieren photographs of the flow about configuration $B_1W_1V_1$ with various tip fin rollout angles at $M = 6.7$ and $\beta = 0^\circ$. At angles of attack below 30°, the shock is seen to intersect the 30° rollout fin, but is outboard at angles of attack of 30° and higher. The effect of this body-shock fin interaction on the directional stability will be discussed later.

Planform Effects at High Sideslip Angles

The effects of wing planform shape on the directional and lateral characteristics at a Mach number of 9.6 were obtained at $\alpha = 0^\circ$ and $\alpha = 10^\circ$ (about $(L/D)_{max}$ for these vehicles); the same trends were observed at both angles of attack. Since the component breakdown tests were conducted only at $\alpha = 0^\circ$, all data are presented for this angle of attack. All four configurations are noted in figure 4 to have negative dihedral effect of about the same magnitude. Removing the vertical tails from configurations $B_1W_1V_1$ and $B_1W_4V_1$ did not appreciably change the rolling moment. This would also be expected of configurations $B_1W_2V_1$ and $B_1W_3V_1$ since the center of pressure of the tails lies very close to the plane of the X-Y axes. With regard to yawing moment, however, wing planform is noted in figure 5 to have an effect. Configurations $B_1W_2V_1$, $B_1W_3V_1$, and $B_1W_4V_1$ are all noted to have a higher level of directional stability C_{n_β} at low sideslip angles than configuration $B_1W_1V_1$. As sideslip angle is increased beyond about 5°, a reduction in the slope or loss of stability is incurred on these three configurations. This reduction in slope is not evident on the full delta-wing configuration $B_1W_1V_1$ or on the tail-off configurations (B_1W_1 and B_1W_4). Plots of side force against sideslip angle are presented in figure 6.

Comparing these results with the schlieren flow photographs in figure 2, it is noted that a reduction in the level of directional stability occurs whenever the body shock intersects the wing leading edge inboard of the tip fin and moves outboard as sideslip angle is increased.

To study this shock interaction in more detail, tests were made with one tail removed; thus the incremental force on each fin could be determined. Figure 7 presents the incremental yawing moment (ΔC_n) and side force (ΔC_Y) for each fin for wing planforms W_1 and W_4 as a function of sideslip angle. In figure 7(b) it is shown that the force and moment acting on the windward fin was essentially unaffected by the differences in wing planform. This is to be expected since the windward fins are operating in a similar flow field. For the leeward fin, however, figure 7(a) shows that a substantial difference in the force and moment characteristics exists with changes in wing planform geometry. On wing W_1 the lee fin is ineffective in producing side force and the incremental yawing moment shown is due only to axial force on the fin. However, on wing W_4 the interaction of the body shock moving outboard along the wing leading edge and crossing over the fin location creates a negative side force at sideslip angles above about 1°. This negative side force produces a positive incremental yawing moment which overcomes the yawing-moment contribution of axial force at an angle of about 5° and results in a positive C_n at higher angles. Since the tail-off and windward-fin yawing moments of $B_1W_1V_1$ and $B_1W_4V_1$ are nearly linear with β and of about the same magnitude and since the axial-force contribution of the windward fin to the yawing moment essentially cancels the input of the lee fin, the change in the yawing-moment-curve slope for the complete vehicle must be attributed to the lee fin and must be created by a shock-interaction effect. In effect, this shock interaction is beneficial in that the directional stability of a cranked-wing vehicle is increased over that for a full delta-wing vehicle at low sideslip angles. However, at higher sideslip angles where the shock moves outboard of the lee fin the shock-interaction effects abate, the cranked-wing vehicle no longer has higher stability than the full delta wing. This shock interaction also accounts for an increase in C_{n_β} between $M = 2.91$ and $M = 6.8$ for configuration $B_1W_4V_1$ as shown in reference 1.

An attempt was made to predict the ΔC_n and ΔC_Y for both fins by use of shock-expansion relationships. These are compared with experimental results in figure 8. Fair agreement was obtained for wing planform W_1, but on W_4 the estimates are not good due to the shock-interaction effects on the lee fin. However, at the higher sideslip angles where the interaction effects are diminished, the experimental data are approaching the theoretical values.

Effects of Tip-Fin Rollout at High Angles of Attack

The effects of fin rollout on the directional and lateral stability characteristics of configuration $B_1W_1V_1$ at $M = 6.7$ are presented as a function of angle of attack in figure 9. Low angle-of-attack data from reference 1 for the configuration with tail off and with 0° fin rollout are also presented as the flagged symbols. By rolling the tip fins outward at high angles of attack, the effective angle of attack of the fin is increased and higher fin effectiveness results. This increased fin effectiveness is due not only to the higher loading at the higher angle of attack but also to the greater rate of change of loading at the higher angle of attack. As seen in figure 9, substantial increases in the level of directional stability are obtained with 15° and 30° fin rollout although the lateral stability parameter C_{l_β} is also increased. Fin rollout will also affect the longitudinal stability of the vehicle and must be taken into account when estimating trim characteristics.

Newtonian estimates of the incremental directional and lateral stability due to rolling out tip fins have been made and the directional stability results have been published in reference 3. Figure 10 presents these estimates along with the experimental values obtained from the present investigation. Fair predictions can be made for 0° rollout angle but at 15° and 30° rollout angle Newtonian theory overestimates the experimental values. Failure of the fins to develop the calculated loads is a result of their operating in a low dynamic pressure, secondary flow field behind the body-wing shock and Newtonian theory should be expected to overestimate the results. Some shock interaction on the tip fin is also noted on the $\phi = 30^\circ$ fin at the lower angles of attack.

CONCLUDING REMARKS

An investigation has been carried out at hypersonic speeds to study the directional and lateral stability characteristics of a winged reentry vehicle at high sideslip angles at a Mach number of 9.6 and at high angles of attack (up to a maximum lift coefficient) at a Mach number of 6.7. The effects of rolling the tip fins out from the vertical were also studied at the higher angles of attack.

It was noted that if the body shock intersects the wing leading edge inboard of the vertical-tip fins higher directional stability results than if the shock was outboard of the fins. However, as sideslip angle is increased and the shock moves outboard of the tip fin, this increase in stability due to the shock interaction on the fin no longer exists and a decrease or loss in positive directional stability

can result. Simple shock-expansion theory gave adequate prediction of the incremental yawing-moment and side-force contributions of the vertical fins for the case where no shock interactions occurred; where shock interaction did occur the theory gave conservative estimates.

At a Mach number of 6.7, rolling the tip fins out 15° and 30° increased the directional-stability level over that for the vertical-tip fins at high angles of attack, but the incremental increase was less than predicted by Newtonian theory. The configuration with vertical-tip fins was directionally stable at all angles of attack up to 60°.

Langley Research Center,
National Aeronautics and Space Administration,
Langley Field, Va., May 3, 1961.

REFERENCES

1. Ladson, Charles L., Johnston, Patrick J., and Trescot, Charles D., Jr.: Effects of Wing Plan-Form Geometry on the Aerodynamic Characteristics of a Hypersonic Glider at Mach Numbers up to 9.6. NASA TM X-286, 1960.

2. Ladson, Charles L., and Johnston, Patrick J.: Aerodynamic Characteristics of Two Winged Reentry Vehicles at Supersonic and Hypersonic Speeds. NASA TM X-346, 1961.

3. Rainey, Robert W., and Close, William H.: Studies of Stability and Control of Winged Reentry Configurations. NASA TM X-327, 1960.

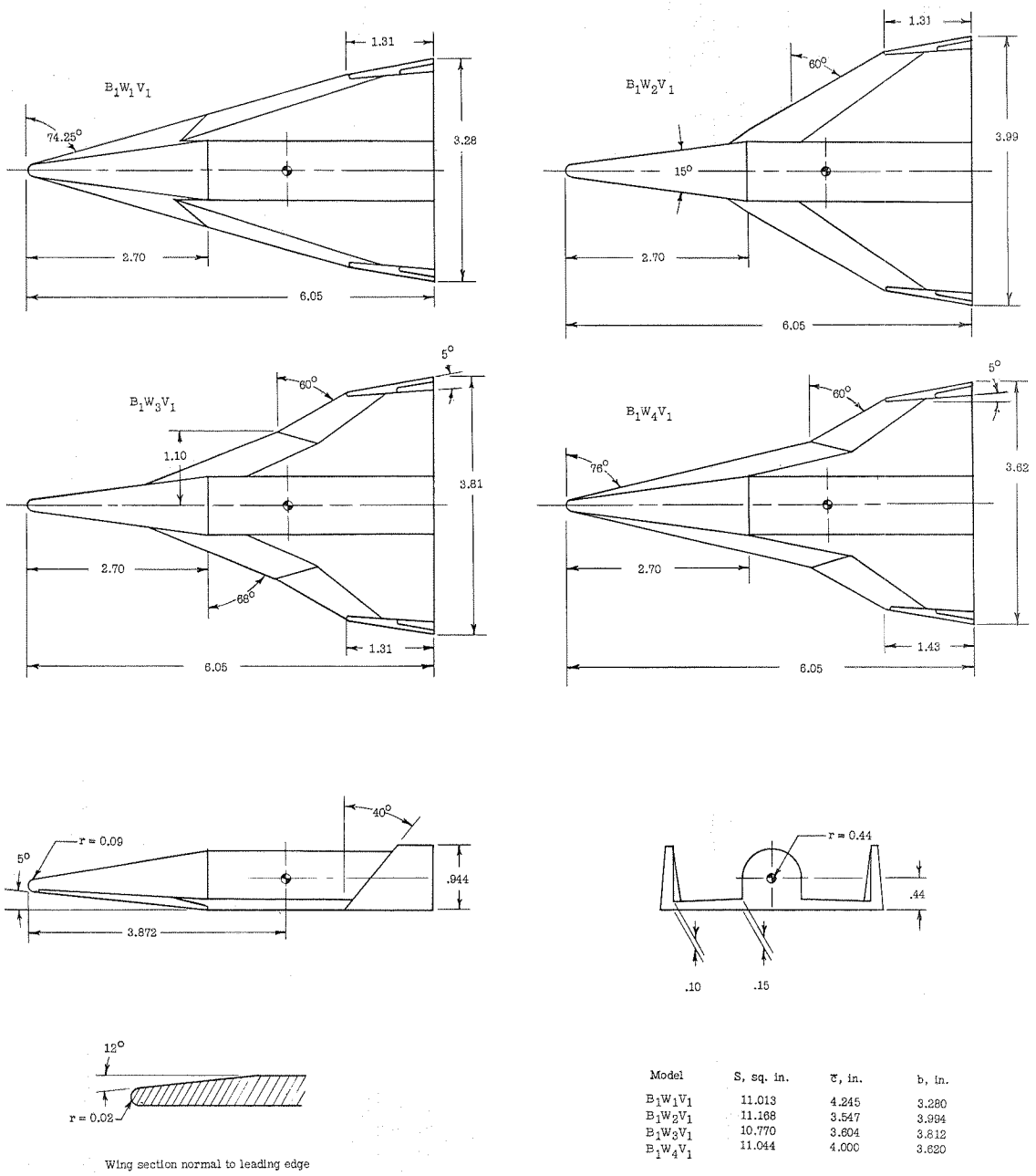

Model	S, sq. in.	$\bar{c}$, in.	b, in.
$B_1W_1V_1$	11.013	4.245	3.280
$B_1W_2V_1$	11.168	3.547	3.994
$B_1W_3V_1$	10.770	3.604	3.812
$B_1W_4V_1$	11.044	4.000	3.620

Figure 1.- Three-view drawings of models tested; all linear dimensions are in inches.

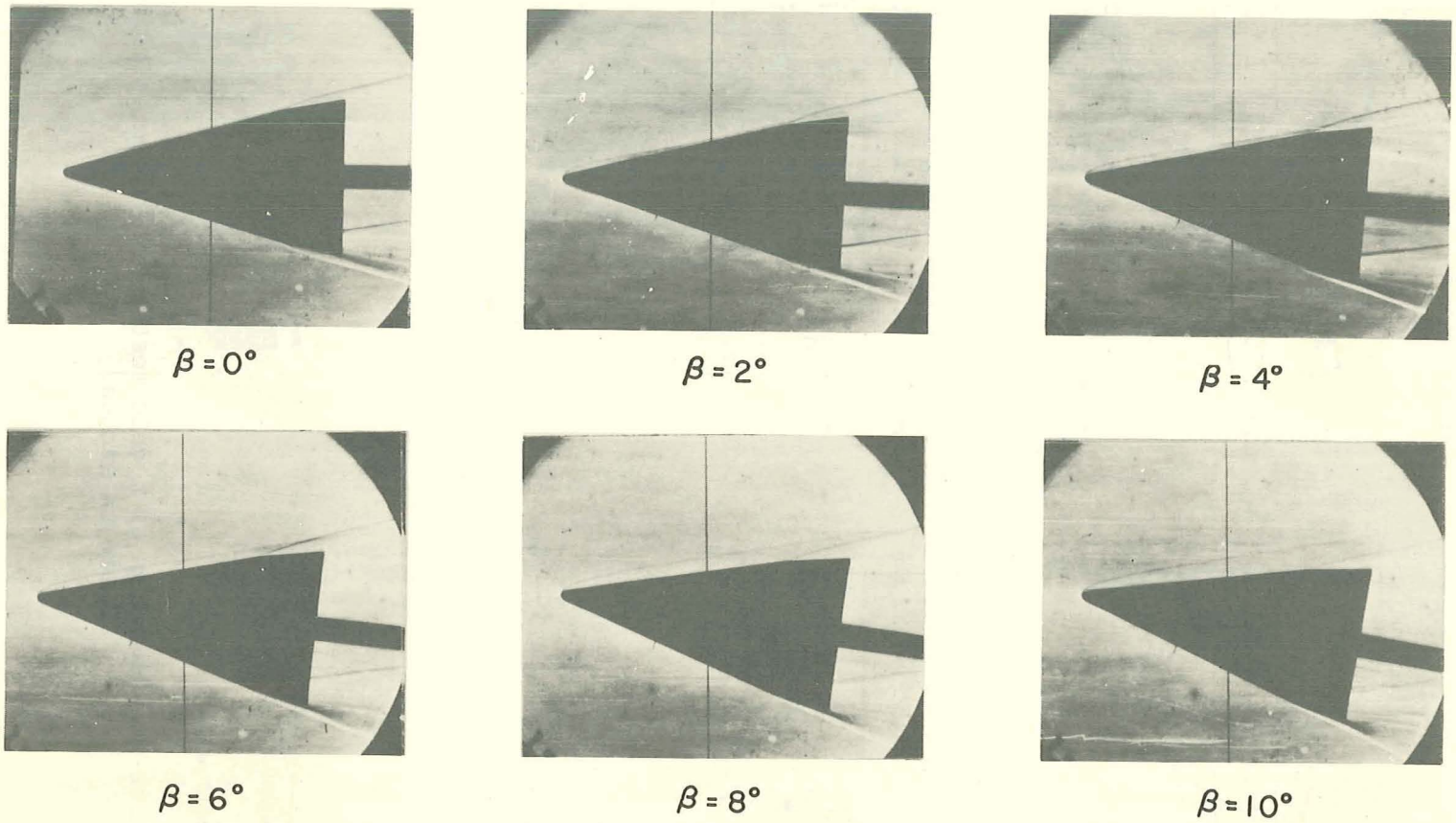

(a) Configuration $B_1W_1V_1$.

L-61-2197

Figure 2.- Schlieren flow photographs at various sideslip angles and 0° angle of attack. M = 9.6.

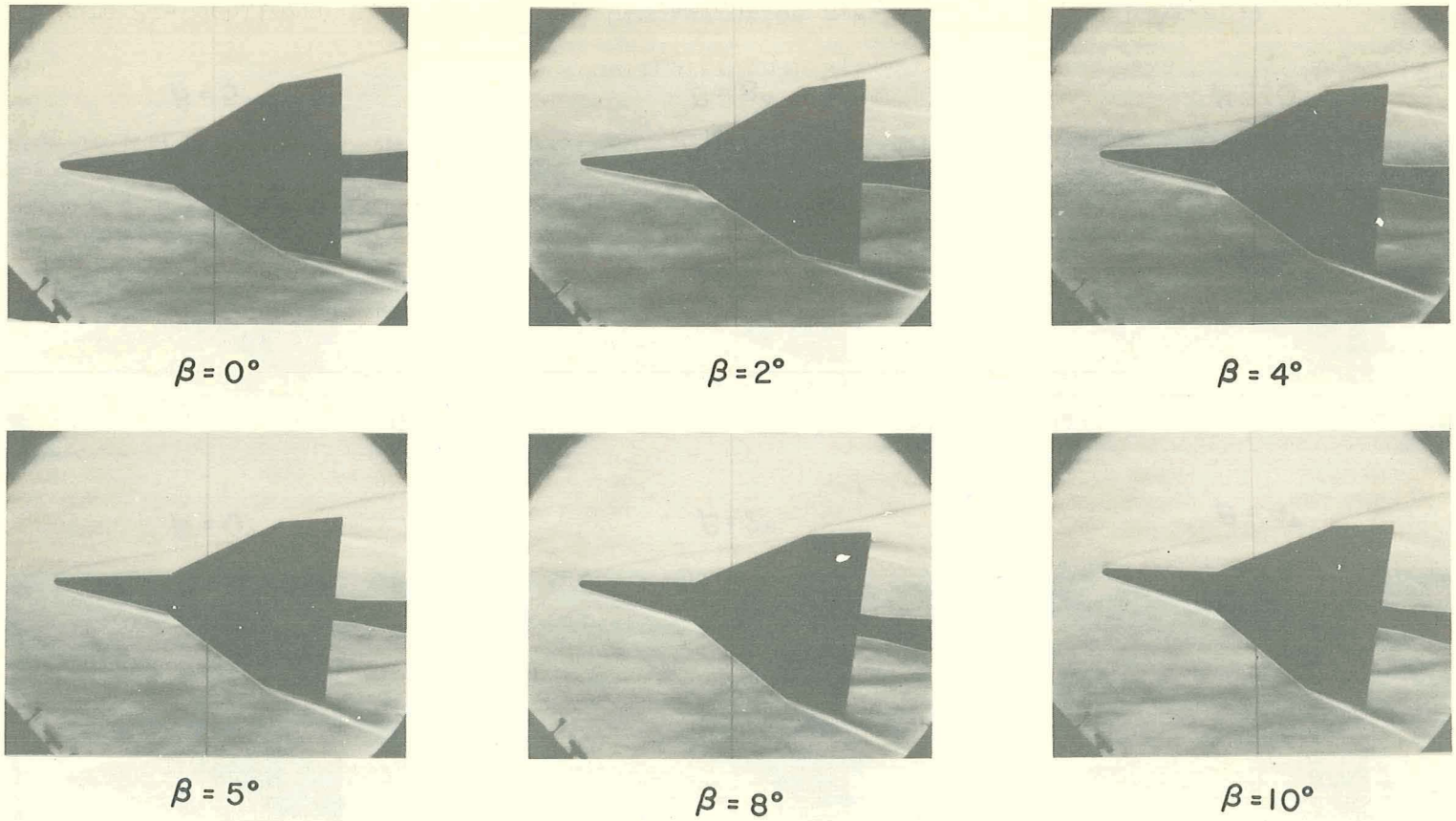

(b) Configuration $B_1W_2V_1$. L-61-2198

Figure 2.- Continued.

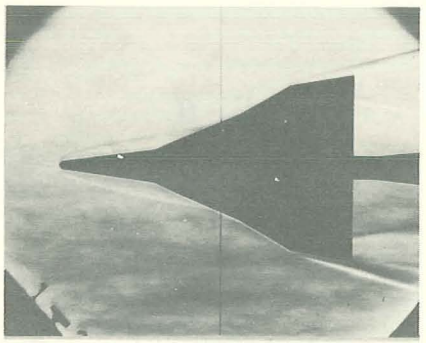

$\beta = 0°$

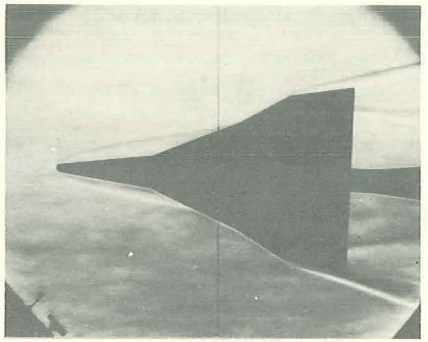

$\beta = 2°$

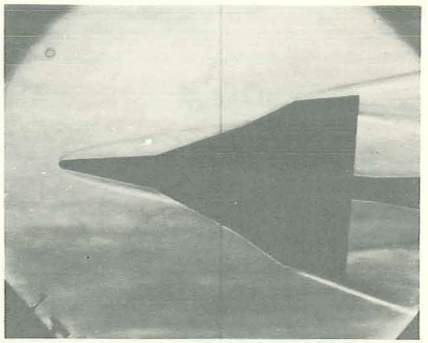

$\beta = 4°$

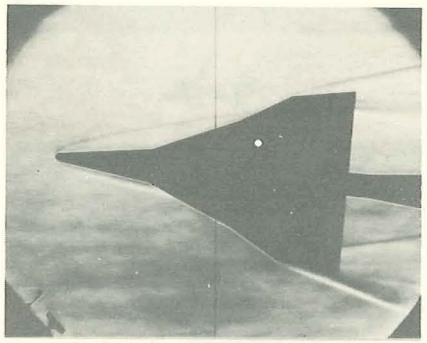

$\beta = 5°$

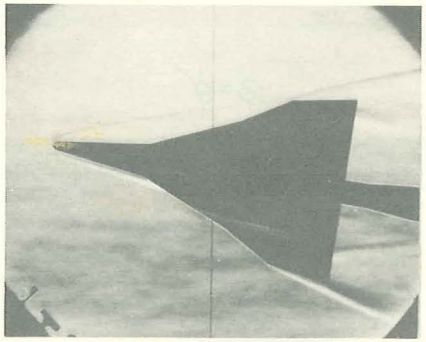

$\beta = 8°$

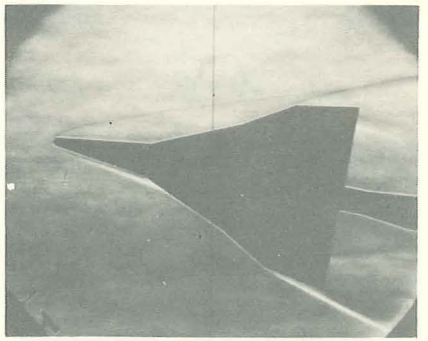

$\beta = 10°$

(c) Configuration $B_1W_3V_1$.

L-61-2199

Figure 2.- Continued.

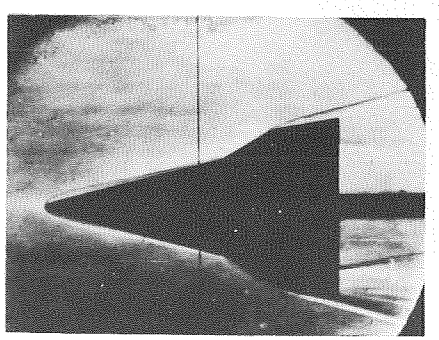

$\beta = 0°$

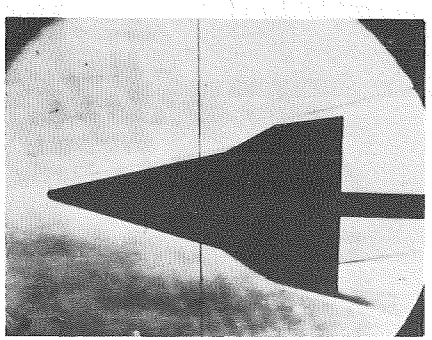

$\beta = 2°$

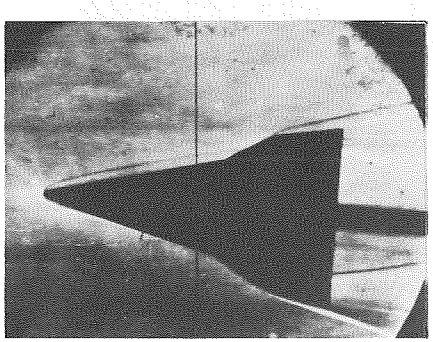

$\beta = 4°$

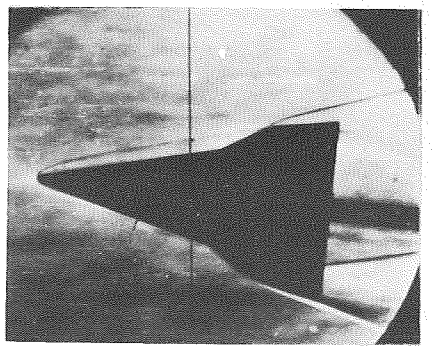

$\beta = 6°$

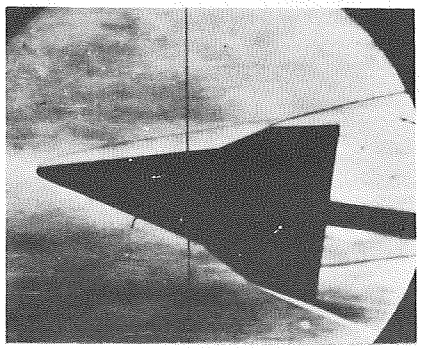

$\beta = 8°$

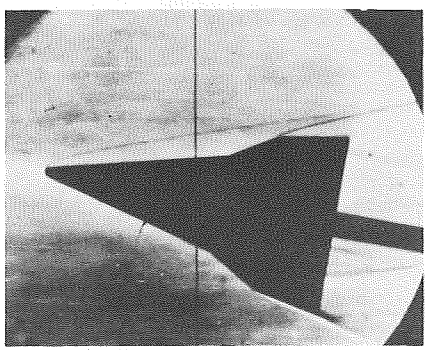

$\beta = 10°$

(d) Configuration $B_1W_4V_1$. L-61-2200

Figure 2.- Concluded.

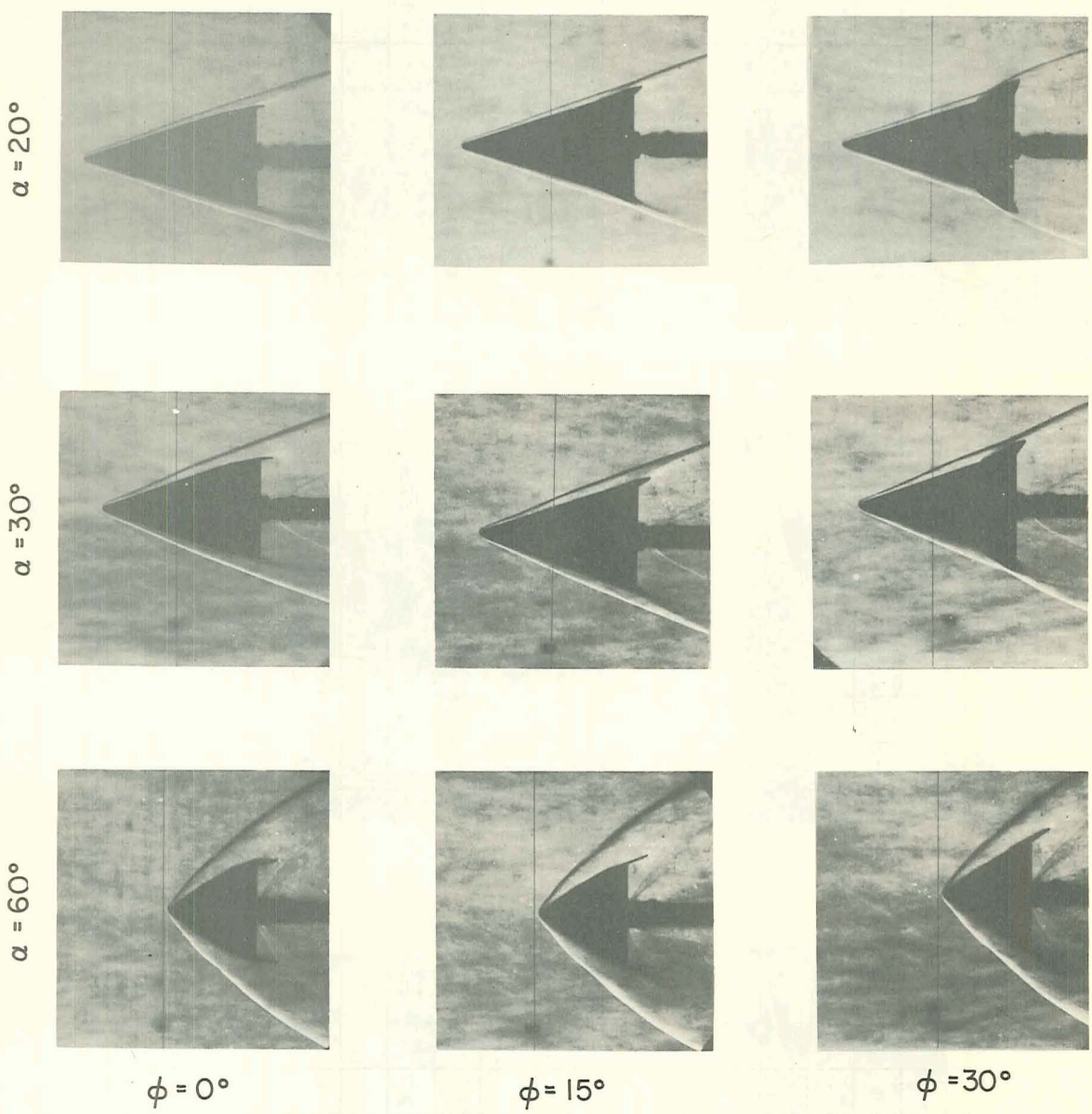

L-61-2201

Figure 3.- Schlieren flow photographs at high angles of attack for several fin rollout angles at $M = 6.7$ and $\beta = 0^{\circ}$ for configuration $B_1W_1V_1$.

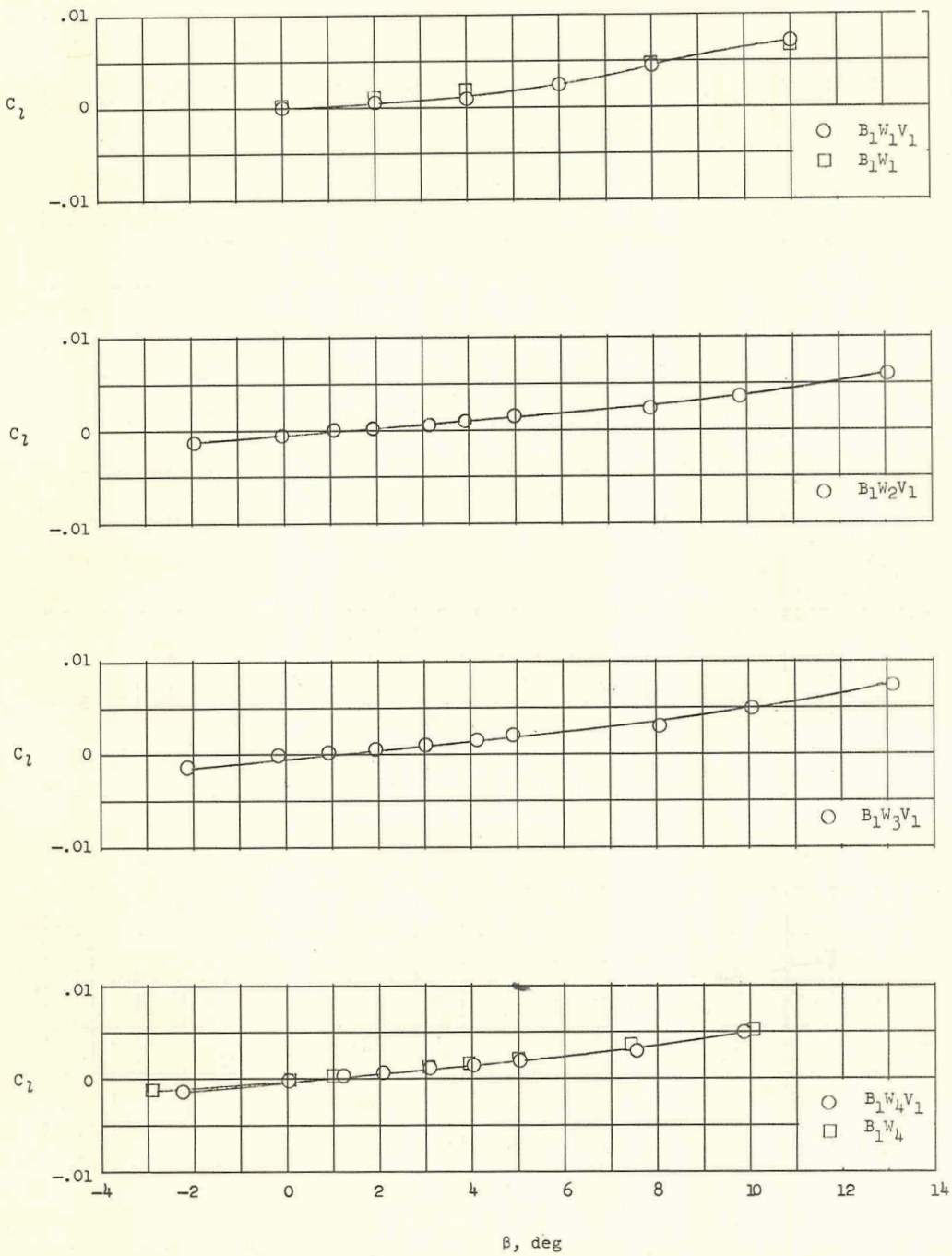

Figure 4.- Rolling-moment characteristics of configurations at high sideslip angles. $\alpha = 0^\circ$; M = 9.6.

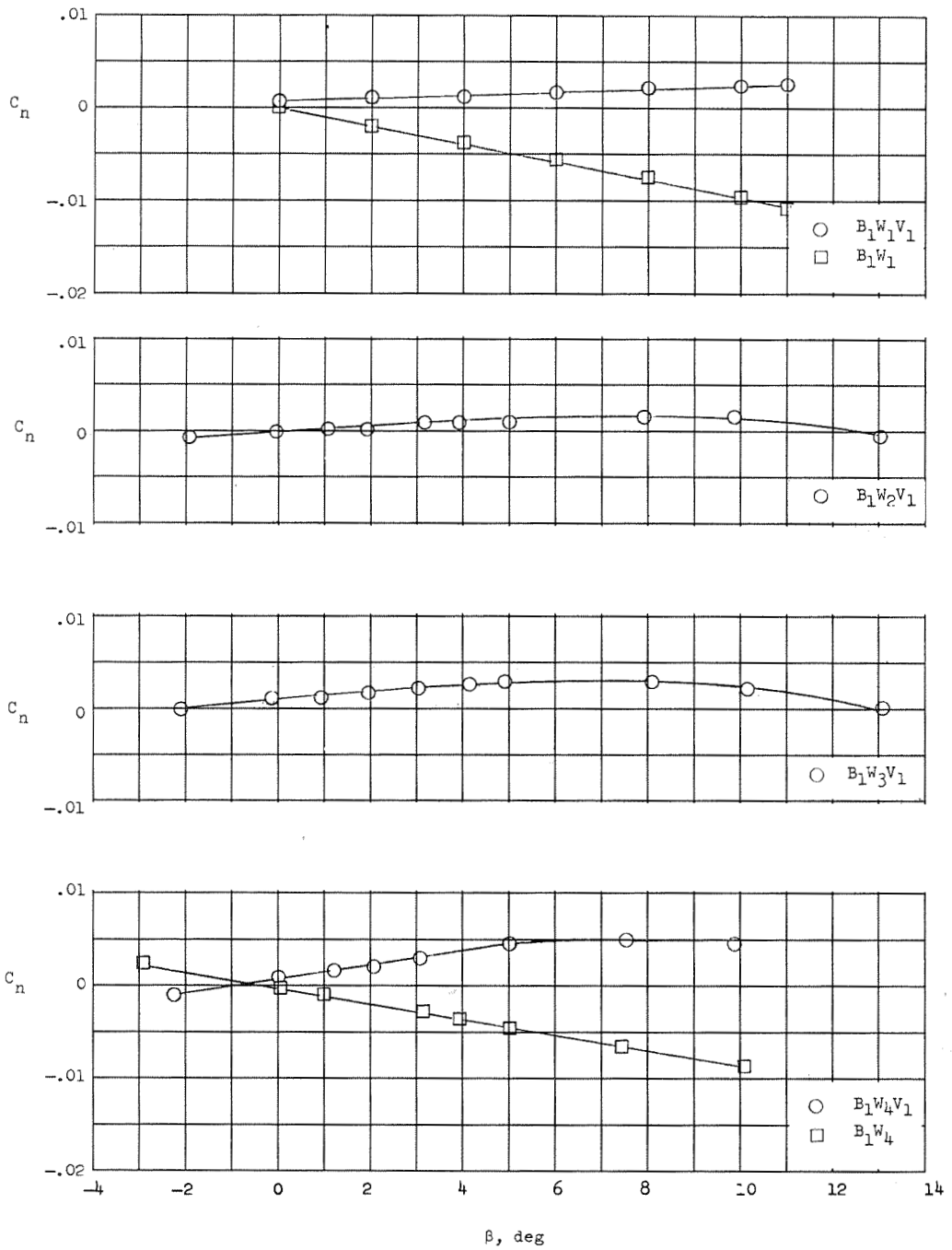

Figure 5.- Yawing-moment characteristics of configurations at high sideslip angles. $\alpha = 0^{\circ}$; M = 9.6.

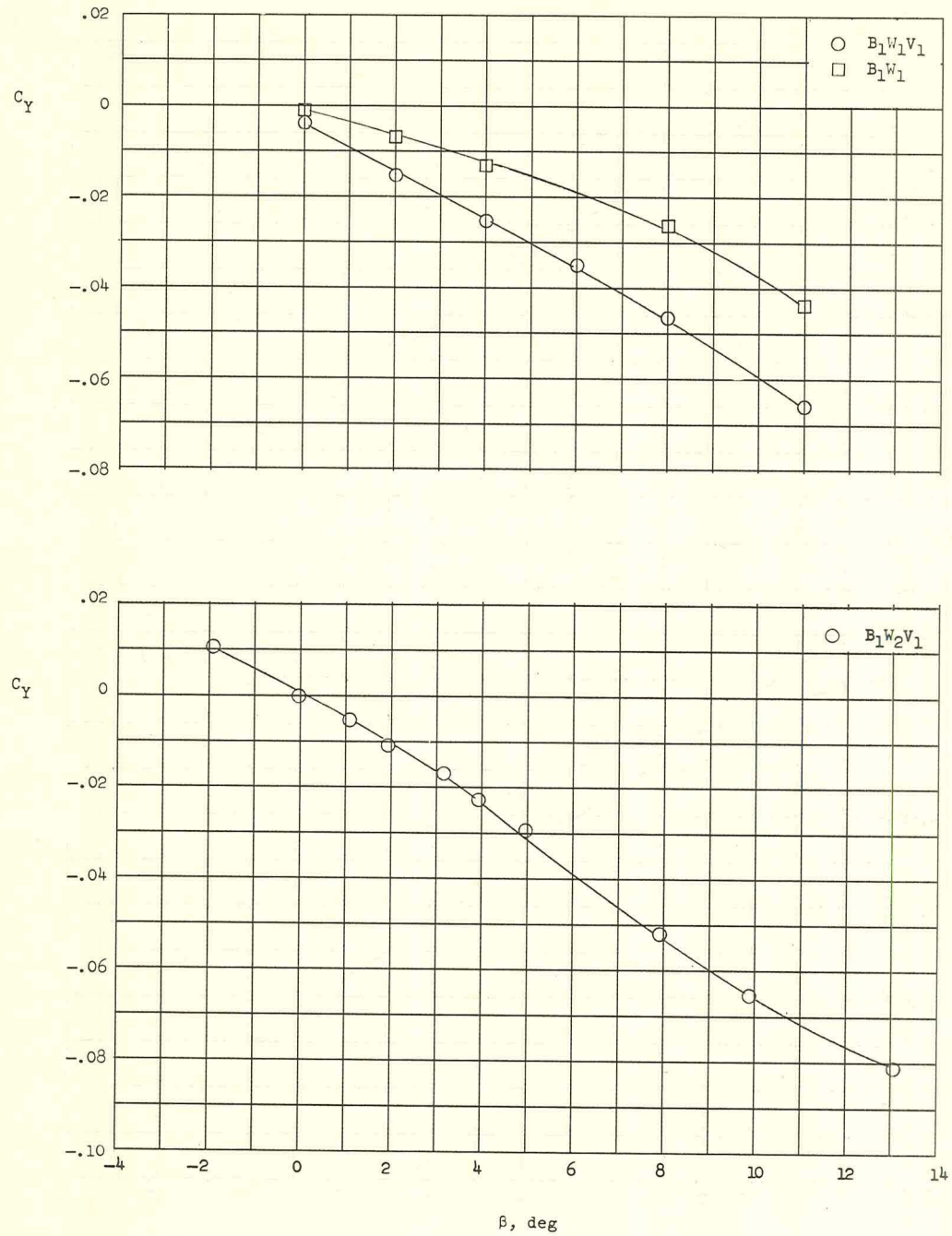

(a) Configurations $B_1W_1V_1$ and $B_1W_2V_1$.

Figure 6.- Side-force characteristics of configurations at high sideslip angles. $\alpha = 0^\circ$; M = 9.6.

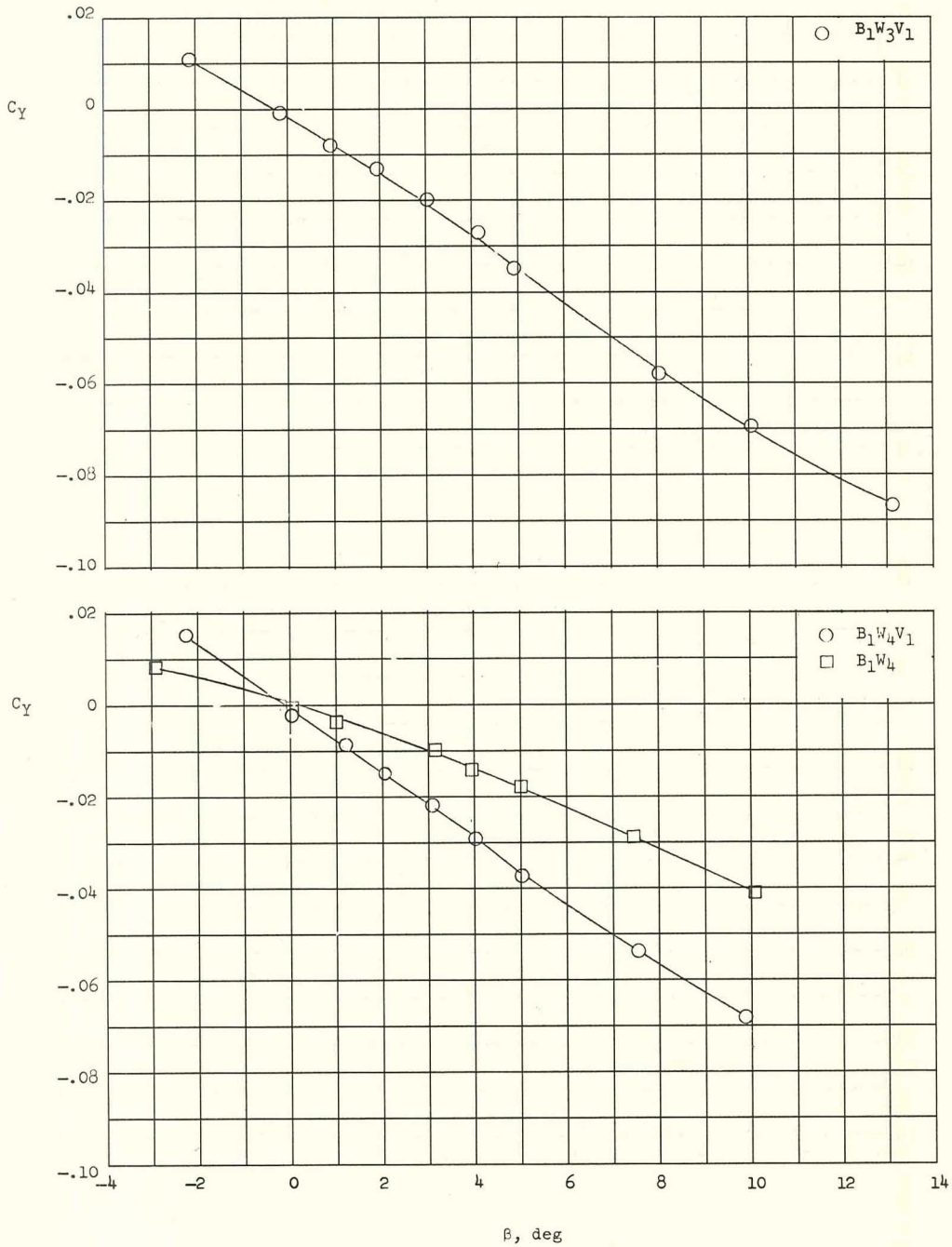

(b) Configurations $B_1W_3V_1$ and $B_1W_4V_1$.

Figure 6.- Concluded.

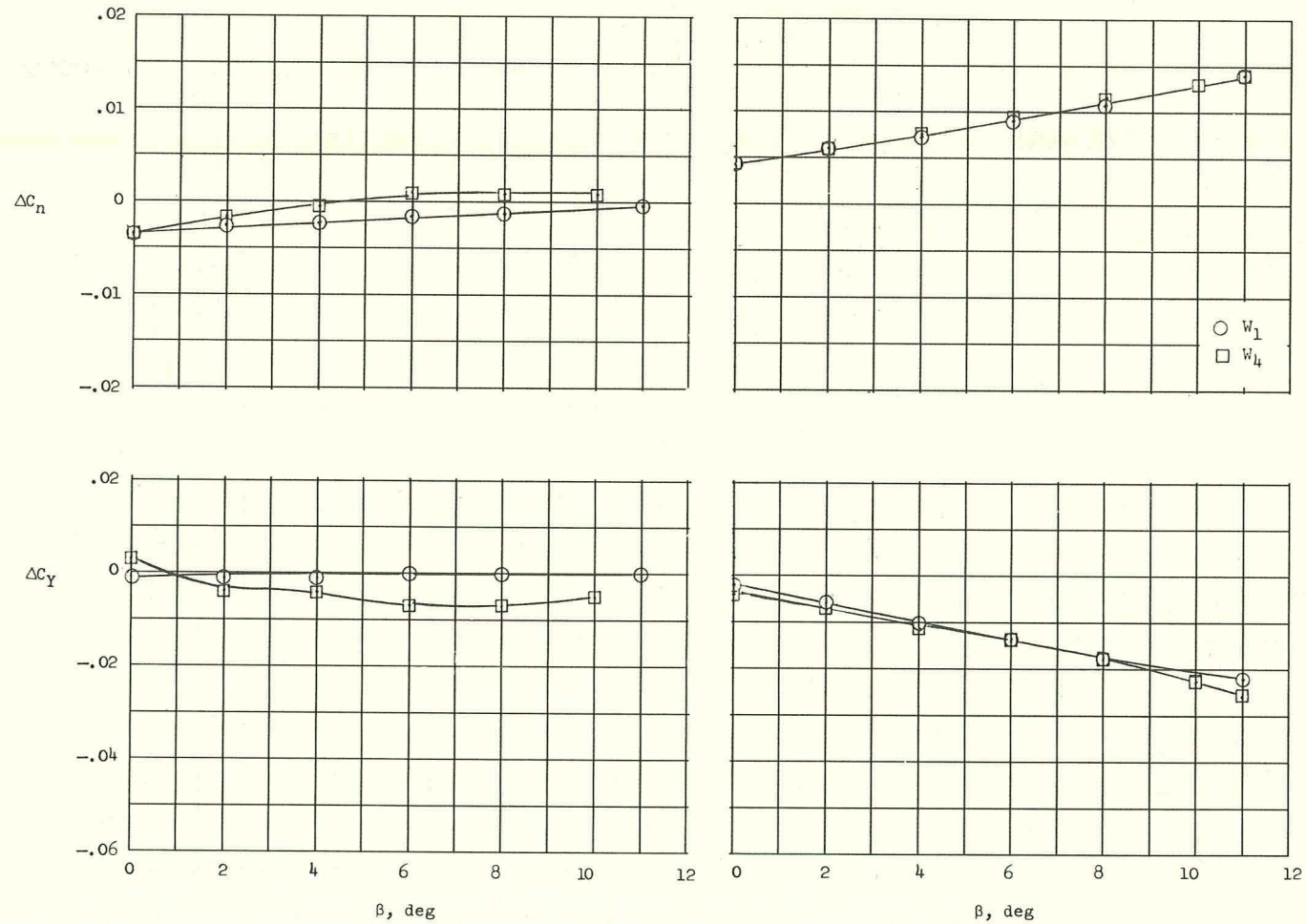

(a) Lee fin.

(b) Windward fin.

Figure 7.- Incremental yawing moment and side force for each fin of configurations $B_1W_1V_1$ and $B_1W_4V_1$. $\alpha = 0^o$; M = 9.6.

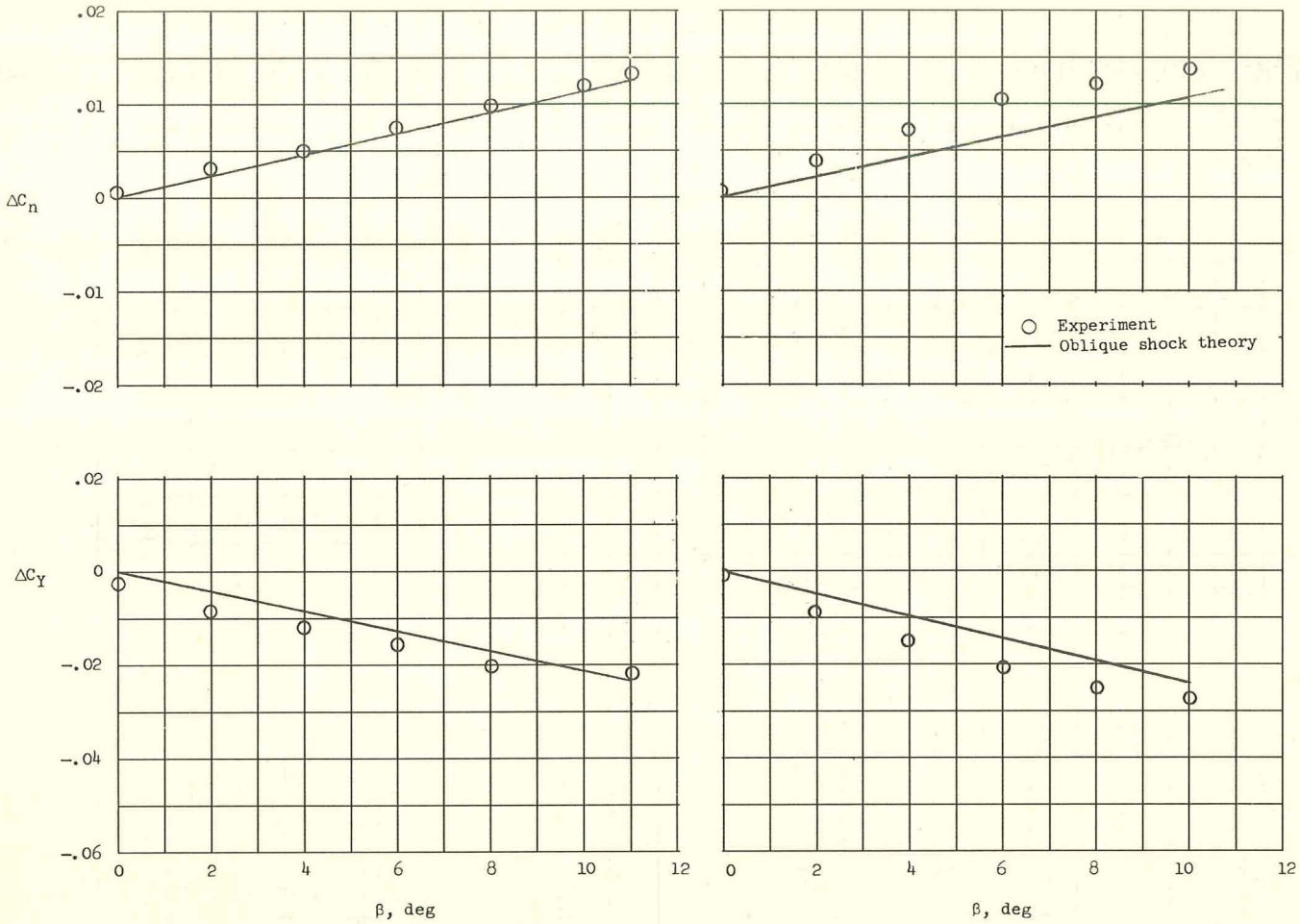

(a) W_1.

(b) W_4.

Figure 8.- Comparison of incremental yawing moment and side force with oblique shock theory. $\alpha = 0^\circ$; M = 9.6.

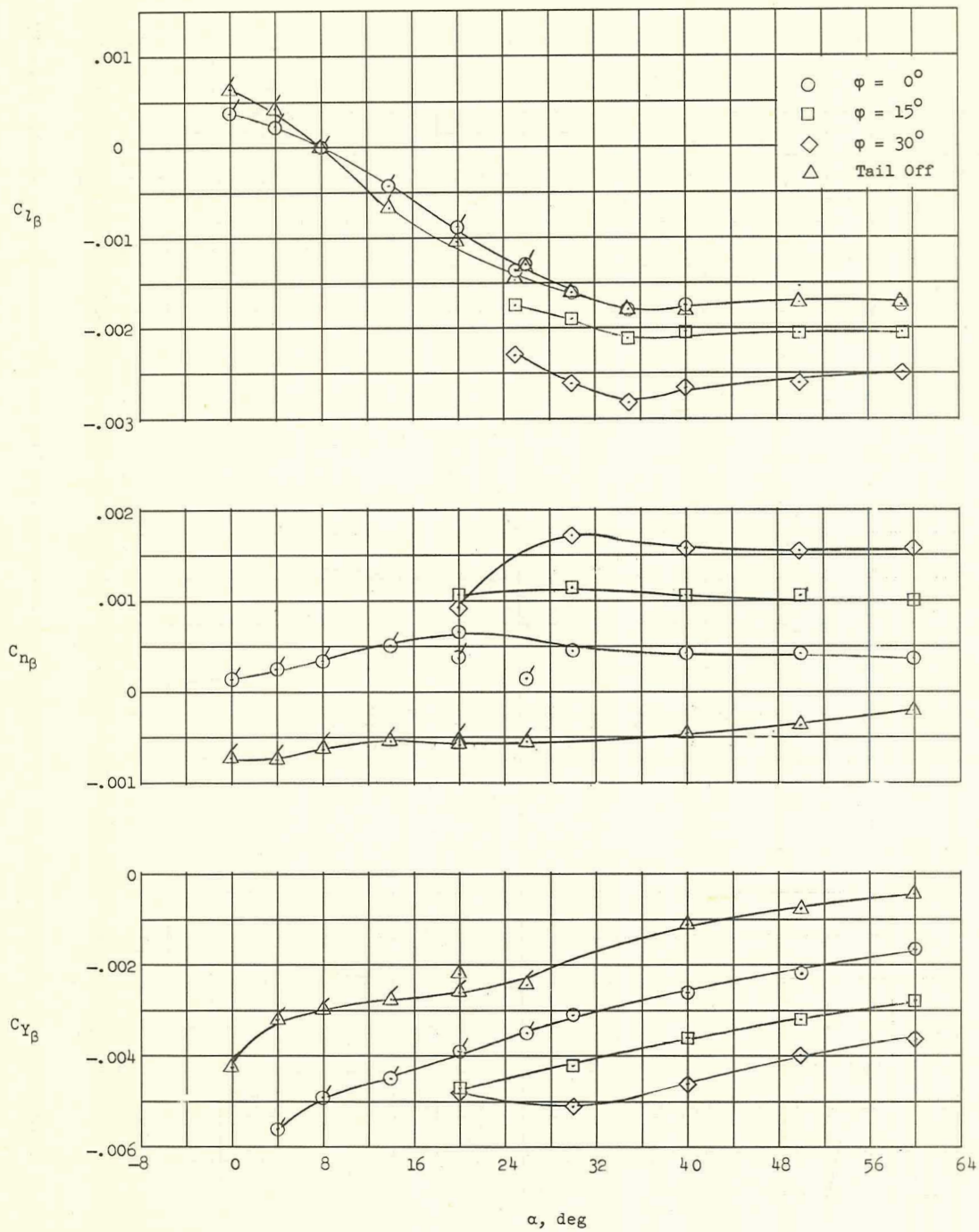

Figure 9.- Effects of vertical-fin rollout on the directional- and lateral-stability characteristics of configuration $B_1W_1V_1$ at M = 6.7. (Flagged symbols taken from ref. 1.)

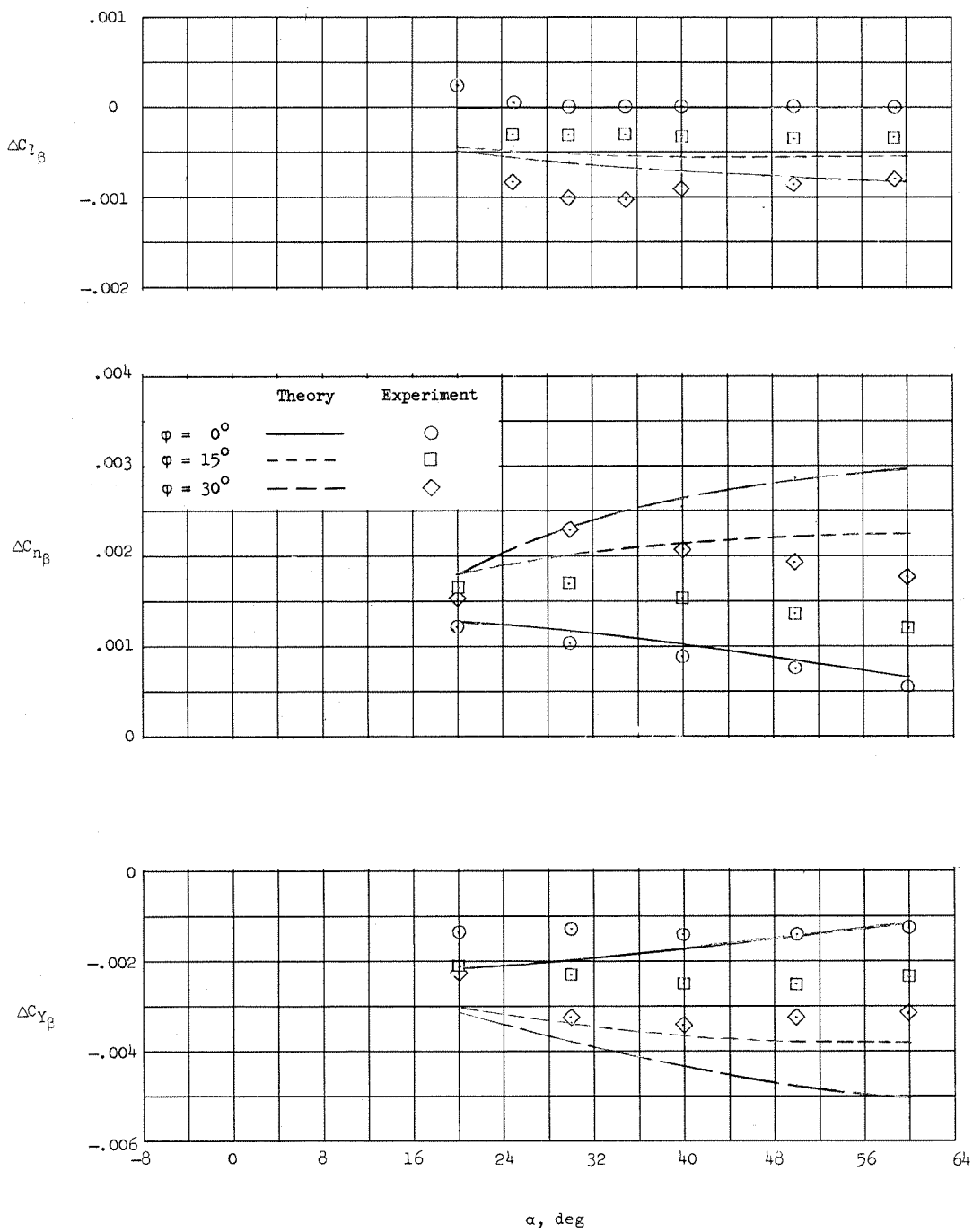

Figure 10.- Comparison of incremental lateral and directional stability due to fin rollout on configuration $B_1W_1V_1$ with Newtonian theory. M = 6.7.

L-1299